

Some practical versions of boundary variation diminishing (BVD) algorithm

Xi Deng^a, Bin Xie^a, Feng Xiao^{a,*}

^a*Department of Mechanical Engineering, Tokyo Institute of Technology,
4259 Nagatsuta Midori-ku, Yokohama, 226-8502, Japan.*

Abstract

This short note presents some variant schemes of boundary variation diminishing (BVD) algorithm in one dimension with the results of numerical tests for linear advection equation to facilitate practical use. In spite of being presented in 1D fashion, all the schemes are simple and easy to implement in multi-dimensions on structured and unstructured grids for nonlinear and system equations.

Keywords:

1. Introduction

Spatial reconstruction schemes under the frameworks of finite volume method (FVM) or finite difference method (FDM) for hyperbolic conservation laws have been extensively exploited in the past decades using high-order-polynomial fashion interpolation functions, see [1] for comprehensive and updated review on the developments in the fields. The polynomial-based high-order (PHO) reconstructions are highly demanded and show excellent performance in resolving numerical solutions which have relatively smooth variations in space, such as acoustic waves and vortices in compressible flow. However, when applied to strong discontinuities, the PHO reconstructions have to be projected to lower order or smoother polynomials (or more precisely rational functions in nonlinear schemes) to suppress numerical oscillations, which is called limiting projection. The limiting projection can be designed by following principles demanded from mathematical or physical perspectives, like the TVD, ENO/WENO and maximum-principle-satisfying. The PHO reconstructions with limiting projection might result in excessive numerical dissipation and tend to smear out the discontinuities in numerical solution. Being aware that the polynomials might not be the best choice in some circumstances for constructing the numerical solution, [8, 9, 10] suggested other non-polynomial functions with better monotonicity-preserving property, like piecewise hyperbolic and piecewise rational reconstructions, which over-perform the polynomial reconstructions in capturing discontinuities with monotone distributions and are able to

*Corresponding author: Dr. F. Xiao (Email: xiao@es.titech.ac.jp)

provide oscillation-less solutions even without limiting projections. However, extending this sort of methods to higher order seems to be not straightforward.

We have shown recently that combining the PHO reconstructions with Sigmoid functions provides a very promising methodology to construct high-fidelity schemes to capture both smooth and jump-like solutions [11, 14, 4, 3]. Implementing such an idea requires some principles or guidelines to hybridize (or switch) the candidate reconstructions according to the numerical solutions. Among other options, we have practiced the boundary variation diminishing (BVD) principle [11] that minimizes the variations (jumps) of the reconstructed values at cell boundaries. The BVD reconstruction effectively reduces the dissipation in numerical fluxes, and thus results in numerical solutions with minimized numerical oscillation and dissipation errors. We have experimented the BVD principle with the 5th-order WENO scheme [2] and the THINC (Tangent of Hyperbola for INterface Capturing) scheme [12, 13, 5, 15], and found that the numerical results of high quality for both smooth and non-smooth solutions can be obtained.

In order to facilitate the practical use of the BVD principle, as well as to promote further exploration for new schemes of better properties, in this note we summarize some simple and efficient BVD algorithms we have tested. Although the discussions are limited to 1D with numerical results only for linear advection test, all algorithms presented here as reconstruction schemes are applicable straightforwardly to multi-dimensions and nonlinear system equations.

2. Preliminary

In this paper, the 1D scalar conservation law in following form is used to introduce the BVD algorithm

$$\frac{\partial q}{\partial t} + \frac{\partial f(q)}{\partial x} = 0, \quad (1)$$

where $q(x, t)$ is the solution function and $f(q)$ is the flux function. We divide the computational domain into N non-overlapping cell elements, $\mathcal{I}_i : x \in [x_{i-1/2}, x_{i+1/2}]$, $i = 1, 2, \dots, N$, with a uniform grid spacing $\Delta x = x_{i+1/2} - x_{i-1/2}$. For a standard finite volume method, the volume-integrated average value $\bar{q}_i(t)$ in cell \mathcal{I}_i is defined as

$$\bar{q}_i(t) \approx \frac{1}{\Delta x} \int_{x_{i-1/2}}^{x_{i+1/2}} q(x, t) dx. \quad (2)$$

The semi-discrete version of Eq. (1) in the finite volume form can be expressed as a ordinary differential equations (ODEs)

$$\frac{\partial \bar{q}_i(t)}{\partial t} = -\frac{1}{\Delta x} (\tilde{f}_{i+1/2} - \tilde{f}_{i-1/2}), \quad (3)$$

where the numerical fluxes \tilde{f} at cell boundaries can be computed by a Riemann solver

$$\tilde{f}_{i+1/2} = f_{i+1/2}^{\text{Riemann}}(q_{i+1/2}^L, q_{i+1/2}^R) \quad (4)$$

if the reconstructed left-side value $q_{i+1/2}^L$ and right-side value $q_{i+1/2}^R$ at cell boundaries are provided. Essentially, the Riemann flux can be written in a canonical form as

$$f_{i+1/2}^{\text{Riemann}}(q_{i+1/2}^L, q_{i+1/2}^R) = \frac{1}{2} (f(q_{i+1/2}^L) + f(q_{i+1/2}^R)) - \frac{|a_{i+1/2}|}{2} (q_{i+1/2}^R - q_{i+1/2}^L), \quad (5)$$

where $a_{i+1/2}$ stands for the characteristic speed of the hyperbolic conservation law. The remaining main task is how to calculate $q_{i+1/2}^L$ and $q_{i+1/2}^R$ through the reconstruction process.

An effective and perhaps the most popular reconstruction scheme is the WENO schemes in which high order but non-oscillatory interpolation is achieved by a combination of several lower degree polynomials. Different variants have been devised following the pioneer works in [7, 6]. In present work, we use the improved 5th-order WENO scheme (WENOZ scheme) proposed in [2] as the PHO reconstruction candidate in the BVD algorithm. Referring the interested readers to [2] for algorithmic details, we denote the 5th-order WENOZ reconstruction function in cell I_i by $q_i^W(x)$, and the cell boundary values are thus computed by $q_i^W(x_{i-1/2})$ and $q_i^W(x_{i+1/2})$ respectively.

We use the THINC scheme [13, 12] as another candidate for reconstruction. Being a Sigmod-type function, the THINC reconstruction (hyperbolic tangent function) is a differentiable and monotone function that fits well a step-like discontinuity. The THINC reconstruction function is written as

$$q_i^T(x) = \bar{q}_{min} + \frac{\bar{q}_{max}}{2} \left(1 + \theta \tanh \left(\beta \left(\frac{x - x_{i-1/2}}{x_{i+1/2} - x_{i-1/2}} - \tilde{x}_i \right) \right) \right), \quad (6)$$

where $\bar{q}_{min} = \min(\bar{q}_{i-1}, \bar{q}_{i+1})$, $\bar{q}_{max} = \max(\bar{q}_{i-1}, \bar{q}_{i+1}) - \bar{q}_{min}$ and $\theta = \text{sgn}(\bar{q}_{i+1} - \bar{q}_{i-1})$. The jump thickness is controlled by parameter β . In our numerical tests shown later a constant value of $\beta = 1.8$ is used, or explicitly stated otherwise. The unknown \tilde{x}_i , which represents the location of the jump center, is computed from $\bar{q}_i = \frac{1}{\Delta x} \int_{x_{i-1/2}}^{x_{i+1/2}} q_i(x)^T dx$. Then the reconstructed values at cell boundaries by THINC function can be expressed by

$$\begin{aligned} q_i^T(x_{i+1/2}) &= \bar{q}_{min} + \frac{\bar{q}_{max}}{2} \left(1 + \theta \frac{\tanh(\beta) + A}{1 + A \tanh(\beta)} \right) \\ q_i^T(x_{i-1/2}) &= \bar{q}_{min} + \frac{\bar{q}_{max}}{2} (1 + \theta A) \end{aligned} \quad (7)$$

where $A = \frac{B/\cosh(\beta)-1}{\tanh(\beta)}$, $B = \exp(\theta \beta(2C - 1))$ and $C = \frac{\bar{q}_i - \bar{q}_{min} + \epsilon}{\bar{q}_{max} + \epsilon}$ with $\epsilon = 10^{-20}$.

3. The BVD algorithms

Given two reconstruction functions shown above, i.e. $q_i^W(x)$ and $q_i^T(x)$, we use the BVD principle to choose the final reconstruction so that $|q_{i+1/2}^R - q_{i+1/2}^L|$ is minimized, which then effectively reduces the numerical dissipation, i.e. the 2nd term in Eq. (5). In this note, we present several BVD algorithms that compare the reconstructed values across cell boundaries. It is noted that we are focusing on the simple and easy-to-use versions of BVD, which are

called in turn BVD(I), BVD(II), BVD(III) and BVD(IV) in this note. Using WENO and THINC as the candidate reconstructions, the resulted schemes are called WENO-THINC-BVD(I) ~ (IV) methods.

3.1. BVD(I) algorithm[11]

- i) Find $q_i^\xi(x)$ and $q_{i+1}^\eta(x)$ with ξ and η being either W or T , so that the boundary variation (BV)

$$BV(q)_{i+\frac{1}{2}} = |q_i^\xi(x_{i+\frac{1}{2}}) - q_{i+1}^\eta(x_{i+\frac{1}{2}})|, \quad (8)$$

is minimized;

- ii) In case that a different choice for cell I_i is made when applying step i) to the neighboring interface $x_{i-\frac{1}{2}}$, that is, $q_i^{\xi'}(x)$ found to minimize

$$BV(q)_{i-\frac{1}{2}} = |q_{i-1}^{\xi'}(x_{i-\frac{1}{2}}) - q_i^{\eta'}(x_{i-\frac{1}{2}})|, \quad (9)$$

with ξ' and η' being either W or T , is different from $q_i^\xi(x)$ found to minimize (8), adopt the following criterion to uniquely determine the reconstruction function.

$$q_i(x) = \begin{cases} q_i^W(x), & \text{if } (q_i^\xi(x_{i+\frac{1}{2}}) - q_{i+1}^\eta(x_{i+\frac{1}{2}}))(q_{i-1}^{\xi'}(x_{i-\frac{1}{2}}) - q_i^{\eta'}(x_{i-\frac{1}{2}})) < 0, \\ q_i^T(x), & \text{otherwise.} \end{cases} \quad (10)$$

- iii) Compute the left-side value $u_{i+\frac{1}{2}}^L$ at $x_{i+\frac{1}{2}}$ and the right-side value $u_{i-\frac{1}{2}}^R$ at $x_{i-\frac{1}{2}}$ by

$$u_{i+\frac{1}{2}}^L = q_i(x_{i+\frac{1}{2}}) \quad \text{and} \quad u_{i-\frac{1}{2}}^R = q_i(x_{i-\frac{1}{2}}). \quad (11)$$

3.2. BVD(II) algorithm[3]

- i) For each reconstruction $q_i^\xi(x)$ with ξ being either W or T , calculate the minimum value of total boundary variation (TBV), $mTBV_i^\xi$, for all possible candidate reconstructions over the neighboring cells by

$$\begin{aligned} mTBV_i^\xi = \min & \left(|q_{i-1}^W(x_{i-\frac{1}{2}}) - q_i^\xi(x_{i-\frac{1}{2}})| + |q_{i+1}^W(x_{i+\frac{1}{2}}) - q_i^\xi(x_{i+\frac{1}{2}})|, \right. \\ & |q_{i-1}^T(x_{i-\frac{1}{2}}) - q_i^\xi(x_{i-\frac{1}{2}})| + |q_{i+1}^T(x_{i+\frac{1}{2}}) - q_i^\xi(x_{i+\frac{1}{2}})|, \\ & |q_{i-1}^W(x_{i-\frac{1}{2}}) - q_i^\xi(x_{i-\frac{1}{2}})| + |q_{i+1}^T(x_{i+\frac{1}{2}}) - q_i^\xi(x_{i+\frac{1}{2}})|, \\ & \left. |q_{i-1}^T(x_{i-\frac{1}{2}}) - q_i^\xi(x_{i-\frac{1}{2}})| + |q_{i+1}^W(x_{i+\frac{1}{2}}) - q_i^\xi(x_{i+\frac{1}{2}})| \right). \end{aligned} \quad (12)$$

- ii) Given the minimum TBVs for both $q_i^W(x)$ and $q_i^T(x)$, $mTBV_i^W$ and $mTBV_i^T$ computed from (12), choose the reconstruction function for cell I_i by

$$q_i(x) = \begin{cases} q_i^T, & \text{if } mTBV_i^T < mTBV_i^W, \\ q_i^W & \text{otherwise} \end{cases}. \quad (13)$$

That is the THINC reconstruction function will be employed in the targeted cell I_i if the minimum TBV value of THINC is smaller than that of high order WENO interpolation.

- iii) Compute the left-side value $u_{i+\frac{1}{2}}^L$ at $x_{i+\frac{1}{2}}$ and the right-side value $u_{i-\frac{1}{2}}^R$ at $x_{i-\frac{1}{2}}$ by

$$u_{i+\frac{1}{2}}^L = q_i(x_{i+\frac{1}{2}}) \text{ and } u_{i-\frac{1}{2}}^R = q_i(x_{i-\frac{1}{2}}). \quad (14)$$

3.3. BVD(III) algorithm [14]

- i) Compute the TBV of the target cell I_i with the WENO reconstruction by

$$TBV_i^{(W)} = \frac{\left(q_{i-1}^W(x_{i-\frac{1}{2}}) - q_i^W(x_{i-\frac{1}{2}})\right)^4 + \left(q_{i+1}^W(x_{i+\frac{1}{2}}) - q_i^W(x_{i+\frac{1}{2}})\right)^4}{(\bar{q}_i - \bar{q}_{i-1})^4 + (\bar{q}_i - \bar{q}_{i+1})^4 + \epsilon}, \quad (15)$$

where ϵ is a small positive of 10^{-16} for avoiding zero-division.

- ii) Compute the smoothness indicator by

$$S = \frac{1 - TBV_i^{(W)}}{\max(TBV_i^{(W)}, \epsilon)}, \quad (16)$$

The cutoff number S_c is used as the threshold value so that the cell where $S < S_c$ is identified to contain a non-smooth solution. We set $S_c = 1 \times 10^6$ here.

- iii) For cell I_i where $S < S_c$, the reconstruction function is determined by blending $q_i(x)^T$ and $q_i(x)^W$ as follows

$$q_i(x) = \omega_i q_i(x)^T + (1 - \omega_i) q_i(x)^W, \quad (17)$$

where ω_i is a weight parameter. By assuming that the WENO reconstruction is applied on neighbor cells, ω_i is obtained by minimizing

$$\tau_i = \left(q_{i-1}^W(x_{i-\frac{1}{2}}) - q_i(x_{i-\frac{1}{2}})\right)^2 + \left(q_{i+1}^W(x_{i+\frac{1}{2}}) - q_i(x_{i+\frac{1}{2}})\right)^2, \quad (18)$$

which leads to

$$\frac{\partial \tau_i}{\partial \omega_i} = 0. \quad (19)$$

As long as ω_i is determined, the reconstruction function $q_i(x)$ is computed from (17).

- iv) Compute the left-side value $u_{i+\frac{1}{2}}^L$ at $x_{i+\frac{1}{2}}$ and the right-side value $u_{i-\frac{1}{2}}^R$ at $x_{i-\frac{1}{2}}$ by

$$u_{i+\frac{1}{2}}^L = q_i(x_{i+\frac{1}{2}}) \text{ and } u_{i-\frac{1}{2}}^R = q_i(x_{i-\frac{1}{2}}). \quad (20)$$

This simplified variant can be easily used for unstructured grids as shown in [14, 4, 16].

3.4. BVD(IV) algorithm

- i) Compute the TBVs of the target cell I_i using WENO and THINC for I_i and its two neighboring cells respectively,

$$TBV_i^W = |q_{i-1}^W(x_{i-\frac{1}{2}}) - q_i^W(x_{i-\frac{1}{2}})| + |q_i^W(x_{i+\frac{1}{2}}) - q_{i+1}^W(x_{i+\frac{1}{2}})| \quad (21)$$

and

$$TBV_i^T = |q_{i-1}^T(x_{i-\frac{1}{2}}) - q_i^T(x_{i-\frac{1}{2}})| + |q_i^T(x_{i+\frac{1}{2}}) - q_{i+1}^T(x_{i+\frac{1}{2}})|. \quad (22)$$

ii) Given TBVs for both $q_i^W(x)$ and $q_i^T(x)$, TBV_i^W and TBV_i^T , choose the reconstruction function for cell \mathcal{I}_i by

$$q_i(x) = \begin{cases} q_i^T & \text{if } TBV_i^T < TBV_i^W, \\ q_i^W & \text{otherwise} \end{cases}. \quad (23)$$

iii) Compute the left-side value $u_{i+\frac{1}{2}}^L$ at $x_{i+\frac{1}{2}}$ and the right-side value $u_{i-\frac{1}{2}}^R$ at $x_{i-\frac{1}{2}}$ by

$$u_{i+\frac{1}{2}}^L = q_i(x_{i+\frac{1}{2}}) \text{ and } u_{i-\frac{1}{2}}^R = q_i(x_{i-\frac{1}{2}}). \quad (24)$$

4. Numerical examples

We show in this section the numerical results of above schemes for advection test. It is noted that when implementing the BVD algorithms presented above we make use the following criteria for choosing THINC reconstruction.

$$\begin{aligned} \delta < C < 1 - \delta, \\ (\bar{q}_{i+1} - \bar{q}_i)(\bar{q}_i - \bar{q}_{i-1}) > 0, \end{aligned} \quad (25)$$

where δ is a small positive 10^{-4} in all numerical tests presented next. Otherwise, the WENO reconstruction is used.

4.1. Advection of One-Dimensional Complex Waves

Proposed in [6], the test of propagation of a complex wave which includes both discontinuous and smooth solutions has been used widely to examine the performance of numerical schemes in solving profiles of different smoothness. The initial distribution of the advected field is set the same as [6]. The numerical result with the WENOZ scheme after one period of computation on a 200-cell mesh is plotted in Fig. 1. Although WENOZ has good performance for smooth region, the discontinuity has been diffused by nearly 8 cells. The smeared discontinuity will become worse for a long time computation.

The numerical results calculated by the WENOZ-THINC-BVD scheme of different BVD algorithms have been shown in Fig. 2–5. All of them can solve discontinuities sharply by nearly 4 cells, which is a significant improvement of present schemes in comparison with those which only use high order polynomials in reconstructions. The result calculated by BVD(I) is presented in Fig. 2. Besides the discontinuous region, BVD(I) also changes the solution around some critical points compared with the original WENOZ scheme. For algorithm BVD(II) as shown in Fig. 3, the numerical result in the smooth regions look almost the same as the original one in Fig. 1, while the numerical dissipation around the discontinuities is remarkably reduced. As one of algorithms devised for unstructured grids, algorithm BVD(III) is capable of solving discontinuities sharply but pollutes smooth regions as shown in Fig. 4,

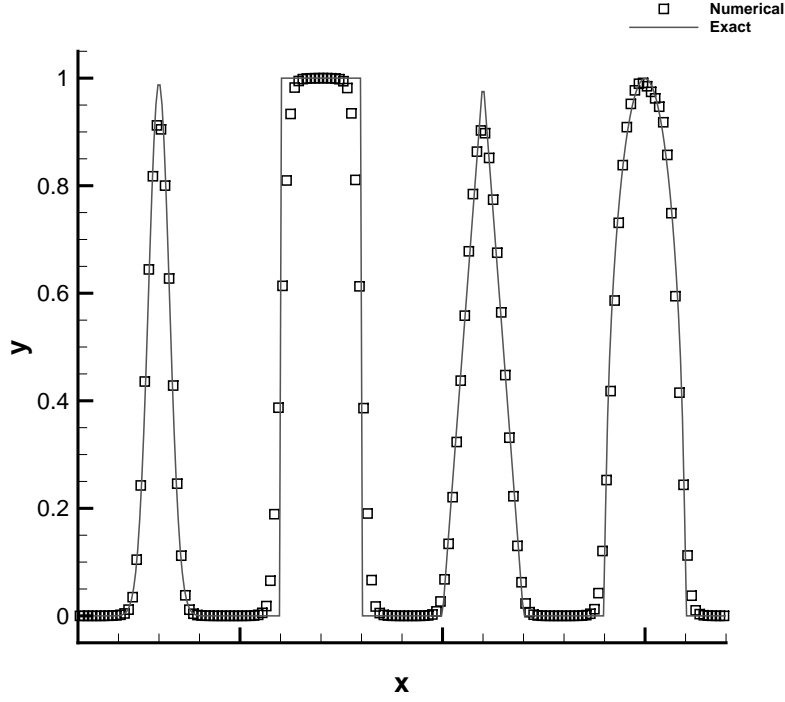


Figure 1: Numerical results of advection of complex waves with the WENOZ scheme.

which may be caused by the assumption that neighbor cells are always smooth. Considering that the discontinuity cannot be resolved by only one cell, BVD(IV) is devised by evaluating TBV with the interpolation function over a group of neighboring cells. Shown in Fig.5, good results comparable to BVD(I) and BVD(II) can be obtained by BVD(IV) which is simple and can be directly implemented on unstructured grids. It is noteworthy that BVD(IV) can use even larger β values. In Fig. 6, we show the result with $\beta = 4.0$ which generates sharper discontinuities resolved by only 2 cells.

5. Conclusion remarks

Acknowledgment

This work was supported in part by JSPS KAKENHI Grant Numbers 15H03916, 15J09915 and 17K18838.

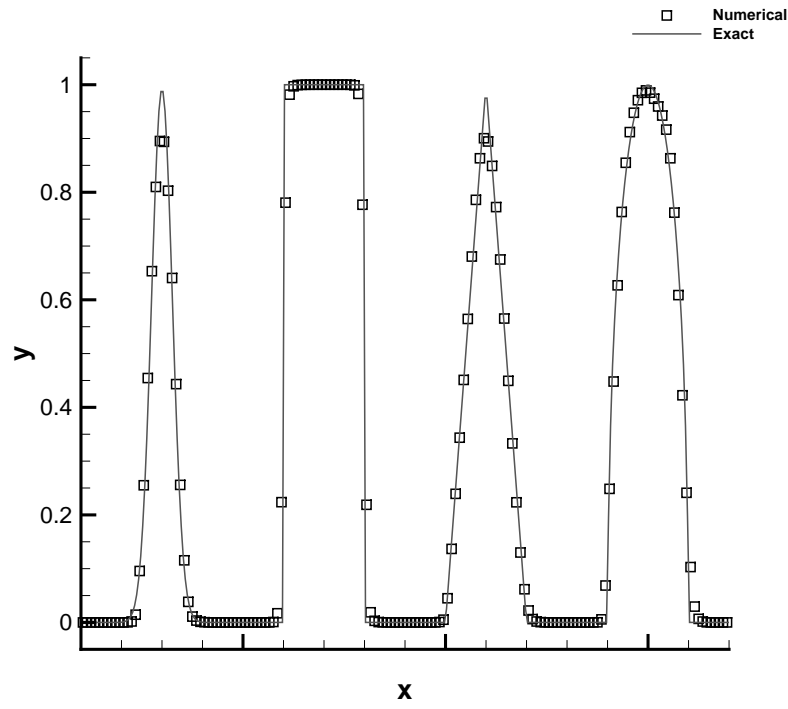


Figure 2: Numerical results of advection of complex waves with the WENOZ-THINC-BVD scheme with BVD(I) algorithm.

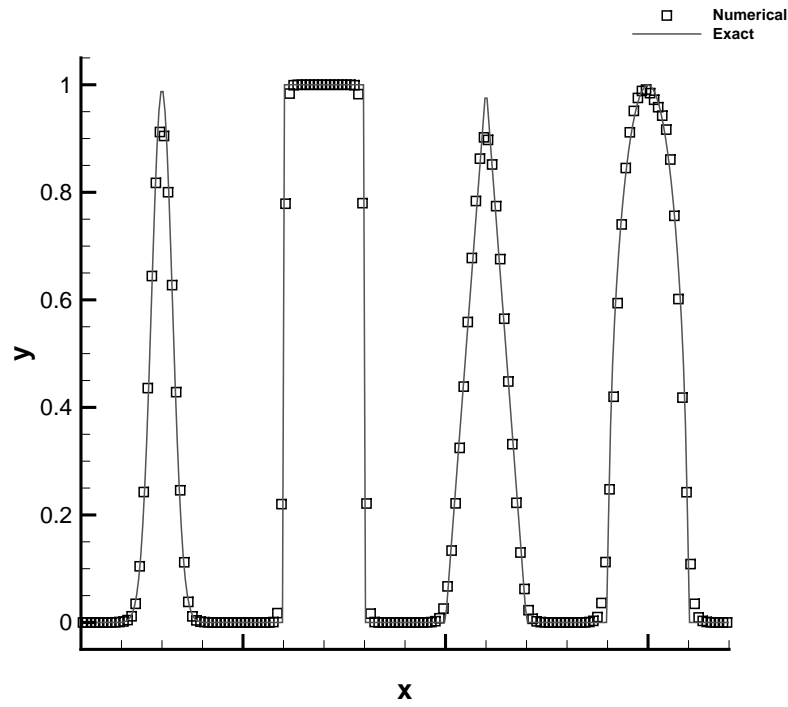


Figure 3: Same as Fig.2, but with BVD(II) algorithm.

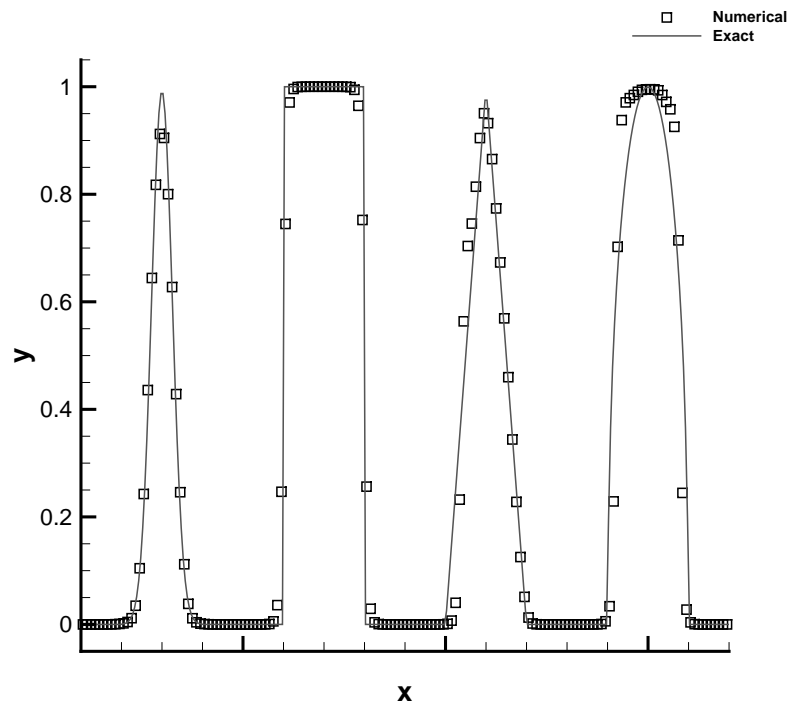


Figure 4: Same as Fig.2, but with BVD(III) algorithm.

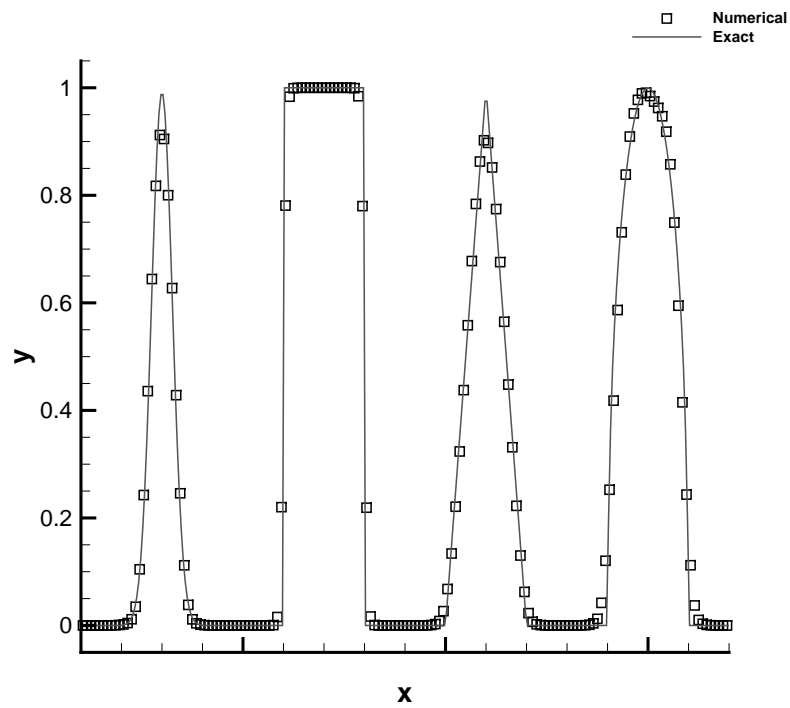


Figure 5: Same as Fig.2, but with BVD(II) algorithm.

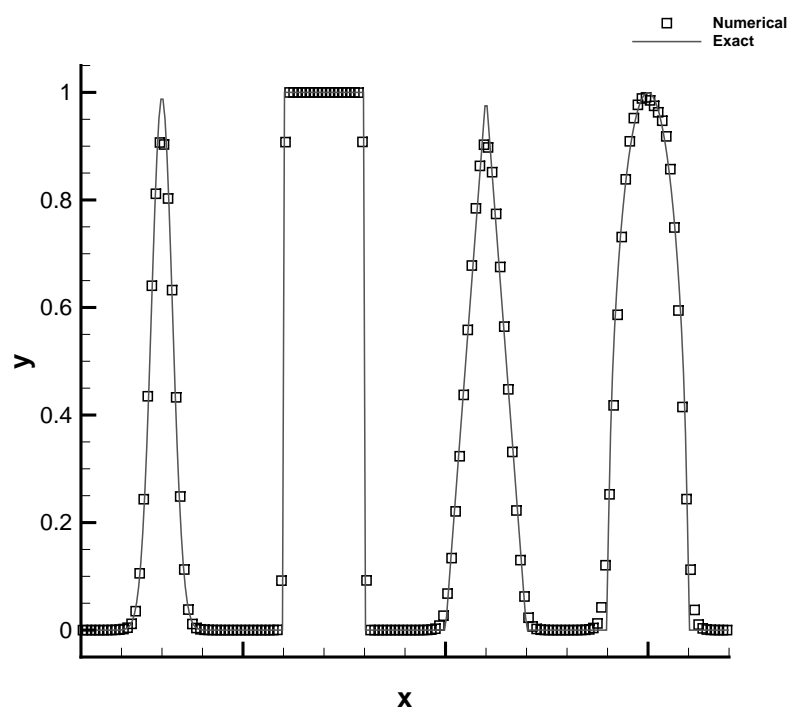


Figure 6: Same as Fig.5, but with $\beta = 4.0$.

References

- [1] Abgrall, Remi, Chi-Wang Shu (ed.). "Handbook of Numerical Methods for Hyperbolic Problems: Basic and Fundamental Issues", Elsevier, 2016.
- [2] Borges, Rafael, Monique Carmona, Bruno Costa, and Wai Sun Don "An improved weighted essentially non-oscillatory scheme for hyperbolic conservation laws." *Journal of Computational Physics* 227.6 (2008): 3191-3211.
- [3] Xi Deng, Satoshi Inaba, Bin Xie, Keh-Ming Shyue and Feng Xiao. "Implementation of BVD (boundary variation diminishing) algorithm in simulations of compressible multiphase flows." *arXiv preprint arXiv:1704.08041*
- [4] Xi Deng, Bin Xie and Feng Xiao. "A finite volume multi-moment method with boundary variation diminishing principle for Euler equation on three-dimensional hybrid unstructured grids." *Computers & Fluids*, 153.10 (2017): 85-101.
- [5] Satoshi Ii, Bin Xie and Feng Xiao, "An interface capturing method with a continuous function: The THINC method on unstructured triangular and tetrahedral meshes." *Journal of Computational Physics* 259 (2014): 260-269.
- [6] Guang-Shan Jiang and Chi-Wang Shu. "Efficient implementation of weighted ENO schemes." *Journal of computational physics* 126.1 (1996): 202-228.
- [7] X.D. Liu, S. Osher and T.F. Chan. "Weighted essentially non-oscillatory schemes." *Journal of computational physics* 115(1994): 200-212.
- [8] Marquina, Antonio. "Local Piecewise Hyperbolic Reconstruction of Numerical Fluxes for Nonlinear Scalar Conservation Laws ." *SIAM Journal on Scientific Computing* 15.4 (1994): 892-915.
- [9] Xiao, Feng and Xindong Peng. "A convexity preserving scheme for conservative advection transport." *Journal of Computational Physics* 198.2(2004): 389-402.
- [10] Artebrant, Robert and H. Joachim Schroll, "Limiter-Free Third Order Logarithmic Reconstruction". *SIAM Journal on Scientific Computing* 28.1 (2006): 359-381.
- [11] Sun, Ziyao, Satoshi Inaba, and Feng Xiao. "Boundary Variation Diminishing (BVD) reconstruction: A new approach to improve Godunov schemes." *Journal of Computational Physics* 322 (2016): 309-325.
- [12] Xiao, F., Y. Honma, and T. Kono. "A simple algebraic interface capturing scheme using hyperbolic tangent function." *International Journal for Numerical Methods in Fluids* 48.9 (2005): 1023-1040.
- [13] Xiao, Feng, Satoshi Ii, and Chungang Chen. "Revisit to the THINC scheme: a simple algebraic VOF algorithm." *Journal of Computational Physics* 230.19 (2011): 7086-7092.
- [14] Xie, Bin, Xi Deng, Ziyao Sun, and Feng Xiao. "A hybrid pressure-density-based Mach uniform algorithm for 2D Euler equations on unstructured grids by using multi-moment finite volume method." *Journal of Computational Physics* 335 (2017): 637-663.
- [15] Bin Xie, Satoshi Ii and Feng Xiao. "An efficient and accurate algebraic interface capturing method for unstructured grids in 2 and 3 dimensions: The THINC method with quadratic surface representation." *International Journal for Numerical Methods in Fluids* 76 (2014): 1025-1042.
- [16] Deng, Xi, Bin Xie, and Feng Xiao. "Multimoment Finite Volume Solver for Euler Equations on Unstructured Grids." *AIAA Journal* (2017).